Palaeogeography, Palaeoclimatology, Palaeoecology 276 (2009) 160–169

Contents lists available at ScienceDirect

Palaeogeography, Palaeoclimatology, Palaeoecology

journal homepage: www.elsevier.com/locate/palaeo

Carbon isotopes and event stratigraphy near the Ordovician–Silurian boundary, Yichang, South China

Junxuan Fan [a,*], Ping'an Peng [b], M.J. Melchin [c]

[a] State Key Laboratory of Palaeobiology and Stratigraphy, Nanjing Institute of Geology and Palaeontology, Chinese Academy of Sciences, Nanjing 210008, China
[b] State Key Laboratory of Organic Geochemistry, Guangzhou Institute of Geochemistry, Chinese Academy of Sciences, Guangzhou 510640, China
[c] Department of Earth Sciences, St. Francis Xavier University, Antigonish, Canada N.S. B2G 2W5

ARTICLE INFO

Article history:
Received 11 April 2008
Received in revised form 9 February 2009
Accepted 2 March 2009

Keywords:
Carbon isotopes
Ordovician–Silurian boundary
Hirnantian
South China
Glaciation
Mass extinction

ABSTRACT

The organic carbon isotope data through the unweathered Ordovician–Silurian boundary strata at the Wangjiawan Riverside section, which is c. 180 m southeast of the Wangjiawan North section, the GSSP for the base of the Hirnantian Stage (Upper Ordovician), show that a positive $\delta^{13}C_{org}$ excursion begins just below the base of the Hirnantian Stage and peaks in the lower part of the *N. extraordinarius* Biozone. This is followed by an interval of slightly reduced $\delta^{13}C$ values and a second peak of 2‰ above pre-Hirnantian values, which occurs in the lower part of the *N. persculptus* Biozone (upper Hirnantian).
The peaks in $\delta^{13}C_{org}$ values can be correlated well with episodes of glacial expansion described from Africa and peri-Gondwanan Europe. Evidence from sedimentological, faunal, and geochemical data from South China, as well as the evidence of glacial sediments in North Africa, all suggests a short-lived glaciation of ~1 Ma in the Ordovician South Pole region, consisting of at least two major pulses. The first phase of gradual glacial expansion began just before the Hirnantian Epoch and the second phase ended with rapid melting in the late Hirnantian (early *N. persculptus* Biozone).

1. Introduction

The Late Ordovician was a time of mass extinction, associated with a widespread continental glaciation that terminated what is widely thought to be a prolonged period of greenhouse climatic conditions (Sheehan, 2001). The mass extinction, the second biggest (in terms of species lost) of the five major events in the Phanerozoic, is estimated to have eliminated 86% of species (Jablonski, 1991). Recent studies from South China also indicate that this event eliminated at least 75% of genera (Rong et al., 2007). Evidence from sedimentological, faunal, and geochemical data all suggests that the major phase of the Late Ordovician glaciation occurred within the early to middle part of the Hirnantian Epoch (e.g., Brenchley et al., 1994; Ghienne, 2003). Carbon isotope chemostratigraphy has become an important tool in the study of bioevents because it can help to constrain the possible nature and range of associated palaeoenvironmental changes, as well provide important markers for global correlation.

The patterns and processes of mass extinction of graptolites (Chen et al., 2004a, 2005; Fan and Chen, 2007) and brachiopods (Rong et al., 2002; Rong and Zhan, 2004) have been described recently based on high-resolution sampling in South China. The biozonation in South China has also been shown to provide a reliable framework for precise correlation of Hirnantian sequences globally (Chen et al., 2006). The present study provides new carbon isotope chemostratigraphic data from the organic matter ($\delta^{13}C_{org}$) from unweathered samples collected in the Yichang area, South China, which are well constrained by graptolite biostratigraphy and are precisely correlated with the described bioevents. These results, combined with carbon isotope data for other palaeoplates, yield new insights into the relative timing of the carbon isotope excursions, the regional and global correlations, and the correlation between faunas and possible environmental changes resulting from the glaciation.

2. Geological setting

Wangjiawan is a small village, 42 km north of Yichang city and the Wangjiawan Riverside section is located at 30°58′28.4″N, 111°25′7.6″E (Fig. 1). It occurs on the east flank of the Huangling Anticline, which has a core of Precambrian rocks. The strata across the Ordovician–Silurian boundary at Wangjiawan include the Wufeng Formation, Kuanyinchiao Bed, and Lungmachi Formation in ascending order. The Wufeng

* Corresponding author. Tel.: +86 25 8328 2183; fax: +86 25 8337 5157.
E-mail addresses: fanjunxuan@yahoo.com (J. Fan), pinganp@gig.ac.cn (P.' Peng), mmelchin@stfx.ca (M.J. Melchin).

0031-0182/$ – see front matter © 2009 Elsevier B.V. All rights reserved.
doi:10.1016/j.palaeo.2009.03.007

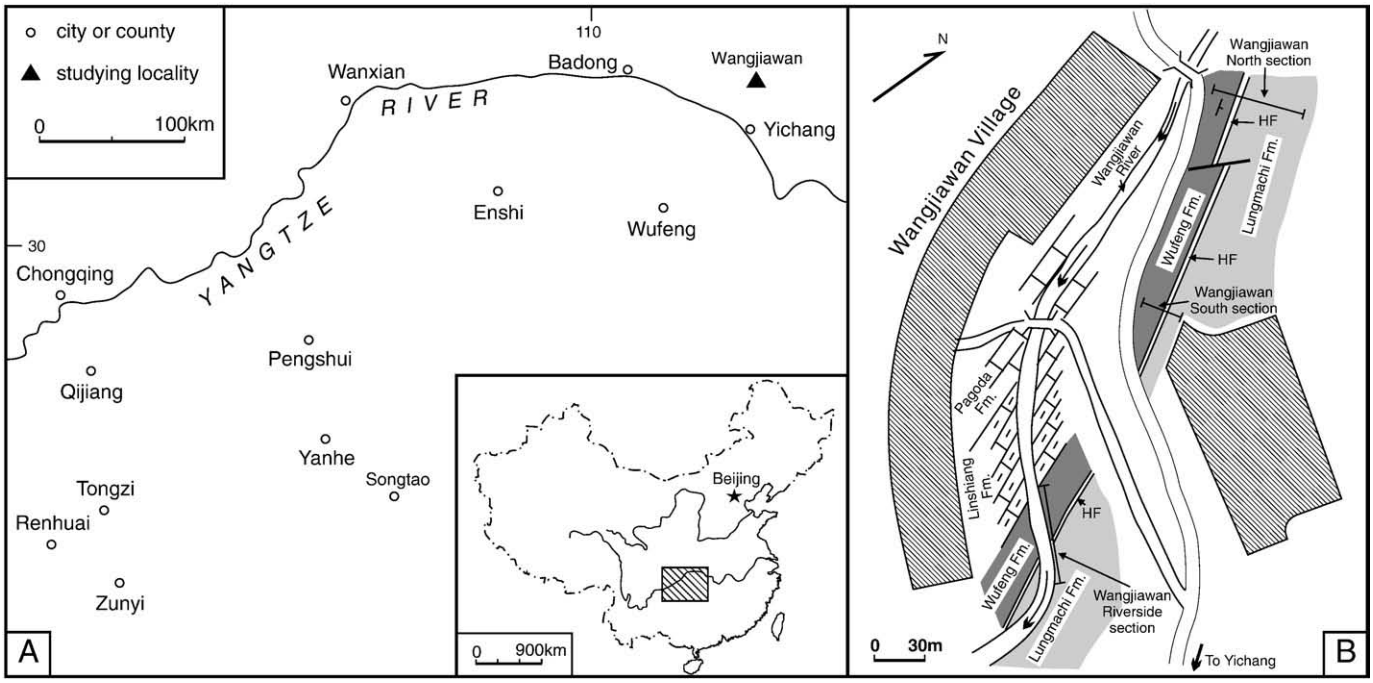

Fig. 1. Map of the study area and a simplified geological map of the Wangjiawan area, Yichang, China (from Chen et al., 2006).

Formation and the Lungmachi Formation at Wangjiawan are characterized by black shales, siliceous shales, and cherts, and yield abundant and diverse graptolite faunas. The Kuanyinchiao Bed is characterized by argillaceous limestone and yields an abundant and diverse shelly fauna, i.e. the *Hirnantia* fauna. The biozonation through these lithostratigraphic units was defined by Mu et al. (1984), Wang et al. (1987) and Mu et al. (1993), and revised by Chen et al. (2000, 2006) (Fig. 2).

The Wangjiawan North section was proposed as the Global Stratotype Section and Point (GSSP) for the base of the Hirnantian Stage by Chen Xu et al. in 2004. The proposal was approved by the Subcommission on Ordovician Stratigraphy in 2005 and by the International Commission of Stratigraphy (ICS) and International Union of Geological Sciences (IUGS) in early 2006 (Chen et al., 2006).

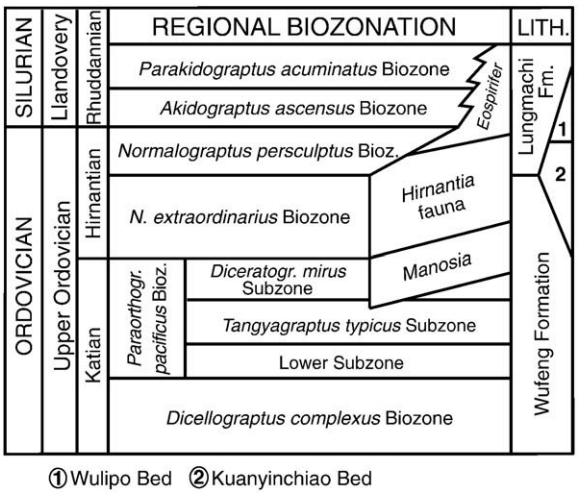

Fig. 2. Upper Ordovician to lowermost Silurian biozonation in South China and its correlation with lithostratigraphic units (from Chen et al., 2006).

3. Materials and methods

The Wangjiawan North and the Wangjiawan South sections yield abundant and diverse graptolites and shelly faunas, but the rocks are intensively weathered. As a result, the organic matter in the strata in those sections can be expected to be significantly altered and degraded, so isotopic analyses of that organic matter may not reliably preserve the original signal. Samples for the present study were collected from the Wangjiawan riverside, *c.* 180 m southeast of the Wangjiawan North section (Fig. 1), which also spans the whole Hirnantian Stage and the Ordovician–Silurian boundary. In this section the rocks are almost unweathered as a result of riverside erosion, so the strata are more suitable for geochemical analysis. Thirty-four samples were collected continuously from the unweathered graptolitic shales (the Wufeng Formation and the Lungmachi Formation) and the argillaceous limestone (the Kuanyinchiao Bed) along the small Wangjiawan River by Fan Junxuan and Peng Ping'an in June of 2005. The sampled interval spans the middle *Paraorthograptus pacificus* Biozone to the *Parakidograptus acuminatus* Biozone and spans two graptolite extinction events (Chen et al., 2005). Each sample is c. 4–9 cm thick.

At present only the organic carbon isotope analysis has been done in the State Key Laboratory of Organic Geochemistry (Guangzhou). About 1 cm was taken off from each face of the samples in order to avoid pollution such as from bacteria or plants. The small samples for the subsequent analysis were picked up from the center of the reduced samples very carefully. The small samples were pulverized into 200 mesh and weighed into pre-cleaned PPCO (polypropylene copolymer) centrifuge tubes. Thirty-five mL of 6M HCl were added and heated at 60 °C for 24 h. During digestion the samples were stirred three times. After digestion the contents were centrifuged for 30 min, and the supernatants were carefully decanted to avoid inadvertent loss. The residue was rinsed four times with 1M HCl. The solid in centrifuge tubes was demineralized with concentrated HCl (6M) + HF (15M) at a volumetric ratio of 1:1 at 60 °C for 24 h. Following centrifuging and rinsing (three times) with 1M HCl, 6M HCl was conducted to remove the minerals in the residue produced during the demineralization procedure. The $\delta^{13}C$ measurements of isolated organic matter were carried out on a Thermo DELTAplus XL

mass spectrometer. The duplicate analyses of every sample were run, and the means of the two measurements were reported in this study (Fig. 3). The standard deviation for six runs of standard BC sample was ±0.1‰.

The graptolites from the same levels were collected and identified by Fan and Chen for each sample. The graptolite biozonation, thus, could be precisely correlated with those of the Wangjiawan North and the Wangjiawan South sections.

4. Results

The $\delta^{13}C$ values vary between −30.3‰ and −30.1‰ through the *Tangyagraptus typicus* Subzone (Fig. 3). It is followed by an increase to −29.5‰ to the upper *Diceratograptus mirus* Subzone. There follows a decline to −29.7‰ in one sample at the base of the *Normalograptus extraordinarius* Biozone. The significance of this single, lowered value is not clear at present. The following $\delta^{13}C$ values become more positive and reach a peak in the middle of the *N. extraordinarius* Biozone with the value of −29.1‰.

The $\delta^{13}C$ value declines slightly to −29.4‰ in the upper part of the *N. extraordinarius* Biozone just below the base of the *Hirnantia* fauna-bearing, argillaceous limestone, the Kuanyinchiao Bed. The $\delta^{13}C$ increases to its highest value (−28.5‰) in the middle of the Kuanyinchiao Bed and then drops to pre-Hirnantian values of −30.3‰ in the upper part of the *N. persculptus* Biozone and then shows minor fluctuation between −30.5‰ and −30.2‰ through the *Akidograptus ascensus* and *Parakidograptus acuminatus* biozones.

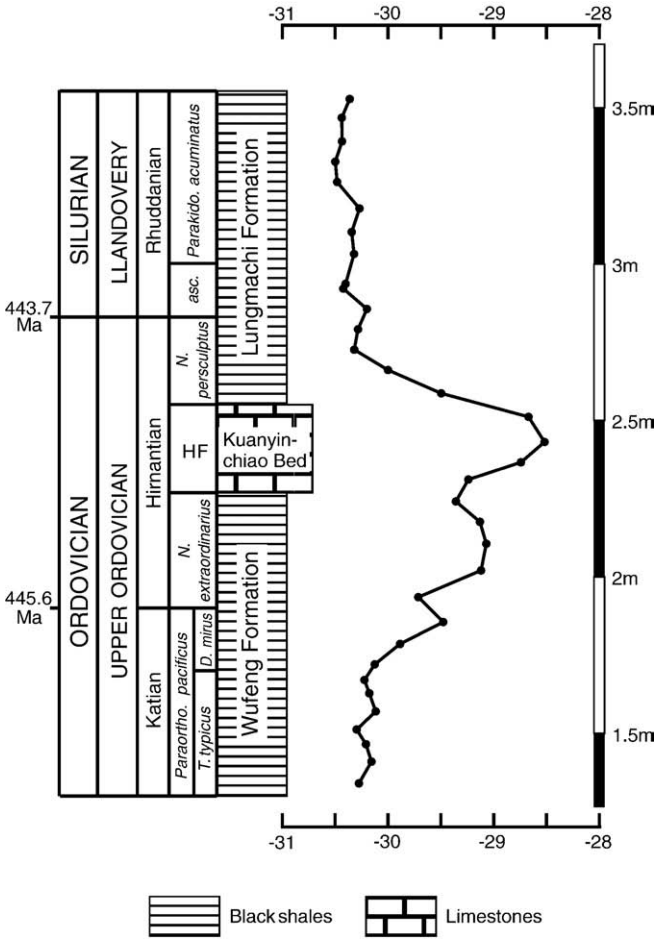

Fig. 3. Organic C-isotope data of isolated kerogen from the Wangjiawan Riverside section with the time scale for Upper Ordovician and lowest Silurian showing Systems, Series, Stages, biozonations and lithostratigraphic units. The absolute ages for the base and top of the Hirnantian Stage come from Cooper and Sadler (2004). HF = *Hirnantia* fauna, asc. = *A. ascensus* Biozone.

5. Regional and global correlations of Hirnantian C-isotope curves

5.1. Regional correlation

By direct biostratigraphic and lithostratigraphic correlation with the nearby Wangjiawan North and South sections, our organic C-isotope curve can be precisely correlated with the regional biozonation (Fig. 3), bioevents (Fig. 4), as well as previously published chemostratigraphic data from this region.

5.1.1. Correlation with previous chemostratigraphic work

Wang et al. (1997) reported a significant positive $\delta^{13}C_{org}$ excursion in the Hirnantian interval at three sections in the Yichang area: Wangjiawan (the Wangjiawan North section of this study), Fenxiang, and Huanghuachang (Fig. 5). More recently, Yan et al. (2009) also reported a similar positive $\delta^{13}C_{org}$ excursion at the Wangjiawan North section, Yichang, Hubei province and the Honghuayuan section, Tongzi, Guizhou province. These data show considerable fluctuation in sample-to-sample $\delta^{13}C_{org}$ values both within and between sections (e.g., the maximum excursion is *c.* 5‰ at Wangjiawan and *c.* 8‰ at Huanghuachang which is only *c.* 13 km from the former site), which is likely the result of the fact that these analyses were conducted on intensely weathered, surface outcrop samples. However, the curves from all three of these sections show some similarity with the data presented here from unweathered samples. In particular, all of these sections show the positive excursion beginning right below the base of the *N. extraordinarius* Biozone (near the base of the *bohemicus* Biozone of Wang et al., 1997), ending within the *N. persculptus* Biozone, and showing peak values within the bed bearing the *Hirnantia* fauna (Fig. 5).

Comparison between the present curve with those from the intensively weathered sections indicates the effect possibly raised by bacteria, modern plants and insects. Because of the humid climate (e.g., the raining season in this area during June and July of every year) and the big Yangtze River crossing this area, the black shale outcrops in the Yichang and neighboring area are commonly covered by grass and bush. All the black shales at the Wangjiawan North, South sections, Fenxiang and Huanghuachang sections are intensively weathered, which are commonly in light yellow or grey, and split into small pieces less than 3 cm thick. The surfaces of these shales are commonly covered by roots of grass and bush; bodies, crusts or empty eggs of some insects are very common in some holes inside the weathered rocks. It is obvious that the present unweathered river-cutted section could provide more reliable signals of the organic carbon isotope excursion.

5.1.2. Timing of the Hirnantia fauna at Wangjiawan

The age of the Hirnantia fauna has been clearly demonstrated to be diachronous in its first and last appearances throughout South China (Rong, 1984a; Rong et al., 2002), which indicates that the base of the overlying Lungmachi Formation may be diachronous throughout South China as well. *N. persculptus* (Elles and Wood) first appears at the base of the Lungmachi Formation at Wangjiawan, however, graphic correlation of Late Ordovician sections throughout South China suggests that the real first appearance of *N. persculptus* (Elles and Wood) in South China possibly correlates within the lower part of the Kuanyinchiao Bed at Wangjiawan (Fig. 4), which indicates that the lower range of *N. persculptus* at Wangjiawan was truncated by the Kuanyinchiao limestones. The Kuanyinchiao Bed at this locality can be correlated with the uppermost part of the *N. extraordinarius* Biozone and the lower part of the *N. persculptus* Biozone. Therefore, the highest $\delta^{13}C$ values, which occur within the Kuanyinchiao Bed, can be correlated to a level within the lower part of the *N. persculptus* Biozone as it is recognized based on the first appearance of *N. persculptus* throughout South China instead of the first appearance of *N. persculptus* at this locality.

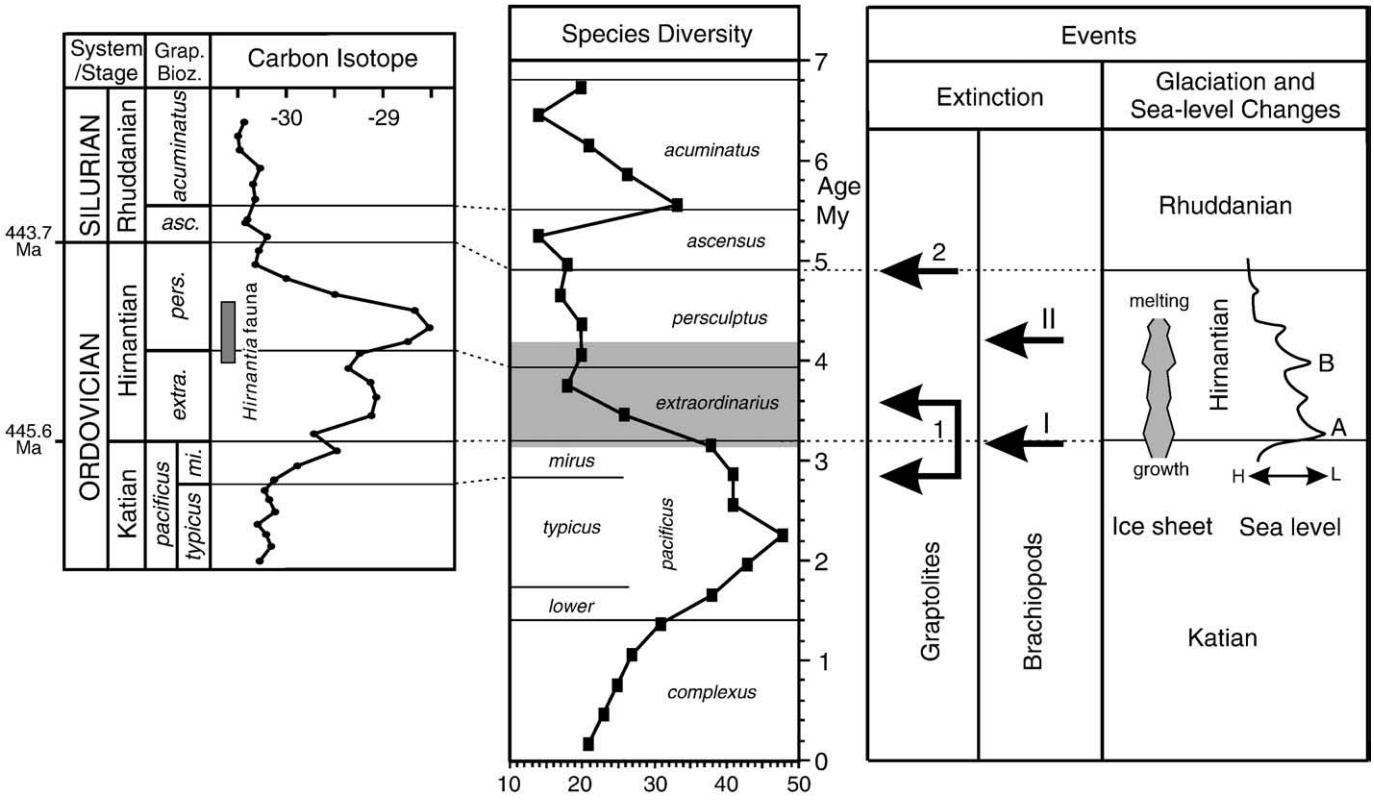

Fig. 4. Correlation of the organic C-isotope curve from the Wangjiawan Riverside section with extinction probability of graptolites (Chen et al., 2005), extinction events of graptolites (Chen et al., 2004a, 2005) and brachiopods (Rong et al., 2002; Rong and Zhan, 2004), Gondwana glaciation and sea-level changes (revised from Ghienne, 2003). Note the correlation of the *Hirnantia* fauna with the two graptolite biozones of Hirnantian Stage at Wangjiawan and the two major pulses of the glacial expansion and sea-level decline (A and B). *pers.* = *N. persculptus* Biozone, *extra.* = *N. extraordinarius* Biozone, *mi.* = *D. mirus* Biozone.

5.1.3. Regional sea-level change and Hirnantian glaciation

The pattern of regional sea-level changes in the Late Ordovician succession in South China can be deduced from several lines of evidence: biofacies changes, lithofacies, and changes in regional paleogeography. A wealth of regional biostratigraphic and paleogeographic evidence from different parts of the world suggests that the most diverse graptolite faunas in any particular time interval occur in slope and deep continental marginal and epicontinental basins (e.g. Cooper et al., 1991; Finney and Berry, 1997; Cooper, 1999). The strata of the *T. typicus* Subzone of the *P. pacificus* Biozone yield the most diverse graptolite fauna in the world for this time interval, including a number of specialized, stenotopic taxa such as *Tangyagraptus, Pseudoretiograptus*, *Paraplegmatograptus* and *Yangzigraptus*. Some of them are endemic to South China (Chen et al., 2005). Chen et al. (2005) suggested that this abundant graptolite fauna represents the radiation of graptolite clades in the warm-water Yangtze epicontinental sea. In the *D. mirus* Subzone of the *P. pacificus* Biozone, the graptolite fauna declines in diversity and co-occurs with the brachiopod *Manosia* and cephalopods, and this assemblage extends into the *N. extraordinarius* Biozone in the Yangtze area, in which graptolite diversity declines further. This is overlain by the argillaceous limestone of the Kuanyinchiao Bed, which yields an abundant shelly fauna including articulate brachiopods, trilobites, and crinoids, but no graptolites, except at some localities in the shallow-water belt in the southwestern Yangtze Platform, such as Honghuayuan, where a low diversity graptolite fauna is associated with the shelly fauna (Chen et al., 2004b). It is considered that the typical *Hirnantia* shelly fauna in Kuanyinchiao Bed in the Yichang area is a relatively shallow water fauna representing Benthic Assemblage 2–3 (BA2-3, *sensu* Boucot, 1975) (Rong, 1979, 1984b; Rong and Chen, 1987; Rong et al., 2002). The changes in regional faunal community appear to represent the transition from BA4-5 in the pre-Hirnantian to BA2-3 of the typical *Hirnantia* fauna (Rong and Chen, 1987; Rong et al., 2002), followed by a return to deeper-water conditions in the overlying black shales of the *N. persculptus* Biozone.

Sedimentary evidence indicates the changing water depth and proximity to the shoreline and sediment source through the study interval. From the upper part of the *T. typicus* Subzone to the *N. extraordinarius* Biozone then to the *Hirnantia* fauna, the lithology changes from fine-grained black shales to yellowish brown shales or mudstones (e.g. the Honghuayuan section, see Fig. 5 in Chen et al., 2000) with coarser clasts, then to argillaceous limestones with a benthic shelly fauna. According to Rong et al. (1984) and Rong and Johnson (1996), at some localities in Guizhou province, which are thought close to the ancient shoreline of the Yangtze epicontinental sea during the Ordovician–Silurian transition, there is an unconformity between the Wufeng Formation and the Lungmachi Formation. This probably indicates the sedimentary affect of the sea level fall during the Hirnantian.

Regional paleogeographic analysis indicates that the Yangtze epicontinental sea was more extensive in pre- and post-Hirnantian time and shrank during the Hirnantian Epoch, particularly during the time of the widespread *Hirnantia* fauna (Chen et al., 2004b).

All of these lines of evidence strongly suggest that the time of deposition of the Kuanyinchiao Bed represented the interval in which sea level was at its lowest in the Late Ordovician succession in the Yichang area.

The typical *Hirnantia* shelly fauna is thought to be a cold/cool-water fauna that developed during the Hirnantian Epoch (Rong et al., 2002), while the Katian shallower *Altaethyrella* and deeper *Foliomena* faunas are thought to be a relatively warm-water fauna (Zhan and Rong, 1995). Accurate correlation of the *Hirnantia* shelly fauna with graptolite

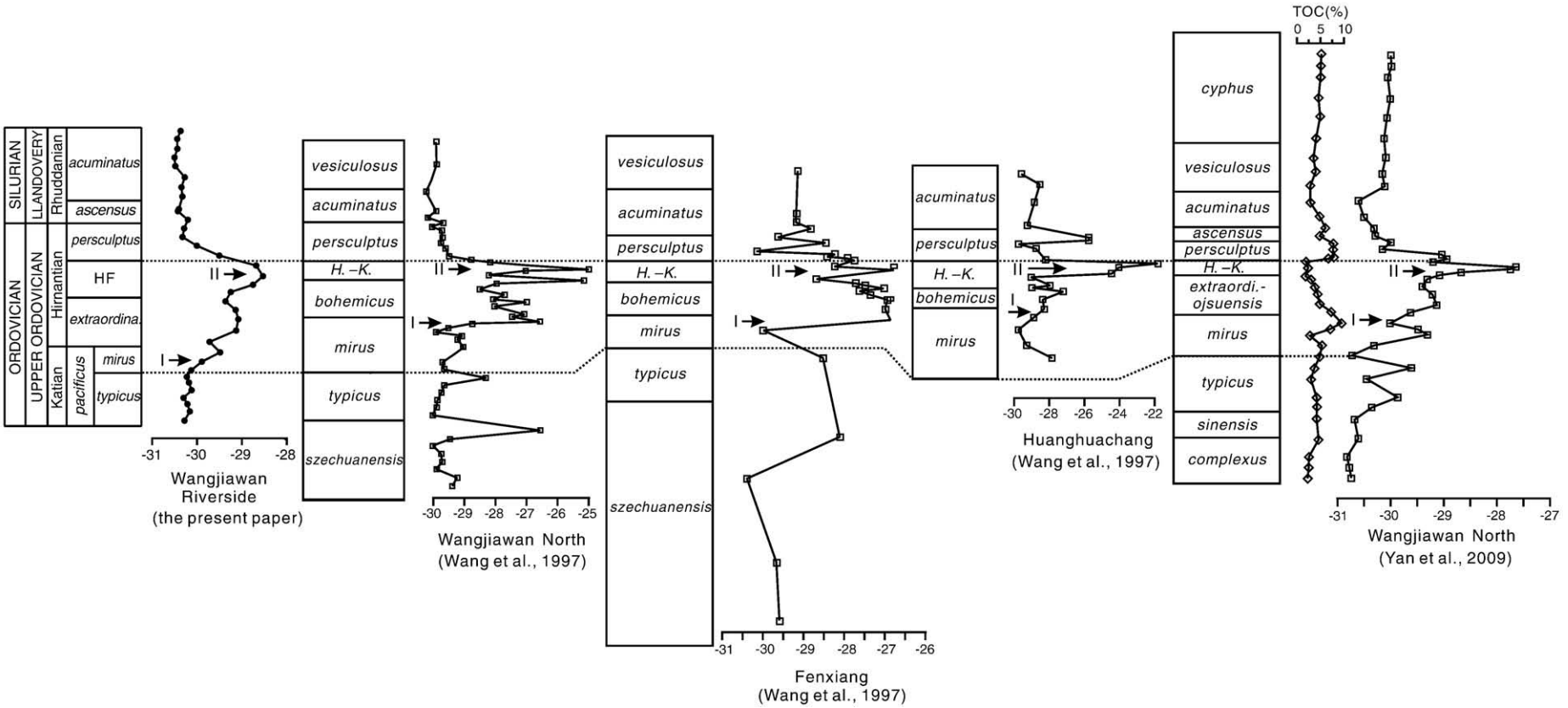

Fig. 5. Correlation with the organic C-isotope curves in Wang et al. (1997) and Yan et al. (2009) and the TOC curve in Yan et al. (2009). Only two correlation lines are given here: the boundary between the Kuanyinchiao limestones (*Hirnantia* fauna) and the overlying Lungmachi graptolitic black shales (*N. persculptus* Biozone), and the first appearance of *Diceratograptus mirus*, the duration of which is very short. The base of the "*bohemicus*" Biozone ("*N. bohemicus*" = *N. ojsuensis*, Fan, 1998) is a little lower than that of the *N. extraordinarius* Biozone (Chen et al., 2006). Two features of the organic carbon isotope curves can be recognized in the four sections, the first (I) indicates the start of the positive excursion in the upper *Paraortho. pacificus* Biozone, and the second (II) indicates the highest peak in the Kuanyinchiao Bed. It is notable that the present study presents a maximum organic carbon excursion of 2‰ while the maximum excursion at Wangjiawan is 3.08‰ in Yan's study and *c.* 5‰ in Wang's study which probably represents the effect of outcrop weathering. HF = *Hirnantia* fauna, *H.–K.*, = *Hirnantia–Kinnella*.

biozonation in South China reveals that both the base and top boundaries of the *Hirnantia* fauna are diachronous. However, Rong et al. (2002) studied the temporal and spatial distribution of the *Hirnantia* brachiopod fauna in South China, Sibumasu, Xizang, and elsewhere. They suggested that, although some key taxa of the *Hirnantia* fauna are present in the upper *P. pacificus* Biozone, the well-defined gradient from low-diversity *Hirnantia* faunas in shallow-water to higher diversity assemblages in offshore, deeper-water environments, first developed in the *N. extraordinarius* Biozone, and most of the fauna disappeared within the *N. persculptus* Biozone (the second phrase of brachiopod extinction, Fig. 4). The ecology of the brachiopod faunas, therefore, appears to show a progressive change from warm water to cooler water in the Yangtze epicontinental sea from Katian to early *N. persculptus* Biozone, coincident with the evidence for sea-level fall.

There is no evidence of a widespread uplift of the South China palaeoplate during this time interval. We believe that both the changes in faunal community and lithology indicate a eustatic sea-level drop from the upper *P. pacificus* Biozone to the upper *N. extraordinarius* Biozone and the lower *N. persculptus* Biozone, which was brought about by the intensification of the Gondwana glaciation.

5.1.4. Correlation with regional bioevents

Chen et al. (2004a, 2005) studied the graptolite mass extinction based on 37 sections in South China. They recognized two extinction events in Late Ordovician, one major extinction event began in the upper *P. pacificus* Biozone and extended through much of the *N. extraordinarius* Biozone (Fig. 4). The second, minor extinction event occurred within the upper part of the *N. persculptus* Biozone. Rong et al. (2002) and Rong and Zhan (2004) also recognized two phases of brachiopod extinction in South China. The first phase is characterized by the elimination of the mid-Ashgill (late Katian) shallower marine *Altaethyrella* and deeper marine *Foliomena* faunas and the invasion of the *Hirnantia* fauna into shallow water regions and this progressively moving into relatively deeper water regimes, starting at the beginning of the Hirnantian Epoch (Zhan and Rong, 1995; Harper and Rong, 1995; Zhan and Cocks, 1998; Rong et al., 1999). The second phase of extinction resulted in the extinction of the *Hirnantia* fauna (Rong and Harper, 1988; Harper and Rong, 1995), which is correlated with the sea level rise in the lower *N. persculptus* Biozone (Fig. 4).

Comparison of the $\delta^{13}C_{org}$ curve with the extinction probability of graptolite species in South China (Fig. 4; Chen et al., 2005) shows that there are some similarities in the profiles from the *P. pacificus* Biozone to the lower *N. persculptus* Biozone. The first positive excursion of $\delta^{13}C$ started from the upper *P. pacificus* Biozone and reached the peak at the mid-*N. extraordinarius* Biozone, which coincides well with the first, major extinction event of graptolites from the upper *P. pacificus* Biozone to the *N. extraordinarius* Biozone as demonstrated by Chen et al. (2004a, 2005), and as well the first phase of the brachiopod extinction just below the Hirnantian Stage (Rong et al., 2002; Fig. 4). The second and higher $\delta^{13}C_{org}$ peak coincides with the incursion of an abundant *Hirnantia–Dalmanitina* fauna, which is mainly a cold/cool-water fauna that lived in a relatively shallow-water environment compared with the pre-existing graptolite fauna (Rong et al., 2002). The following dramatic drop of the $\delta^{13}C_{org}$ values is consistent with the extinction of this widespread shelly fauna (Rong et al., 2002), the cause of which is thought to be a rapid melting of the Gondwana ice sheet, sea level rise, global warming, and flood of many deep shelf regions with anoxic waters. This level is also coincident with a significant rise in graptolite origination rates (Chen et al., 2005).

5.2. Global correlation

The $\delta^{13}C$ data have been previously published from a number of sections around the world, including Estonia and Latvia (Brenchley et al., 2003, carbonate), Scotland (Underwood et al., 1997, organic carbon), Anticosti Island, Canada (Long, 1993, carbonate), Arctic Canada (Melchin and Holmden, 2006, organic carbon and carbonate), and Nevada, USA (Finney et al., 1999, carbonate; Mitchell et al., 2007, carbonate and organic carbon). Among these known sections, the Wangjiawan Riverside section provides a high-resolution correlation with graptolite succession, typical *Hirnantia* fauna, and sea-level change, and thus plays an important role in global correlation of $\delta^{13}C$ curves.

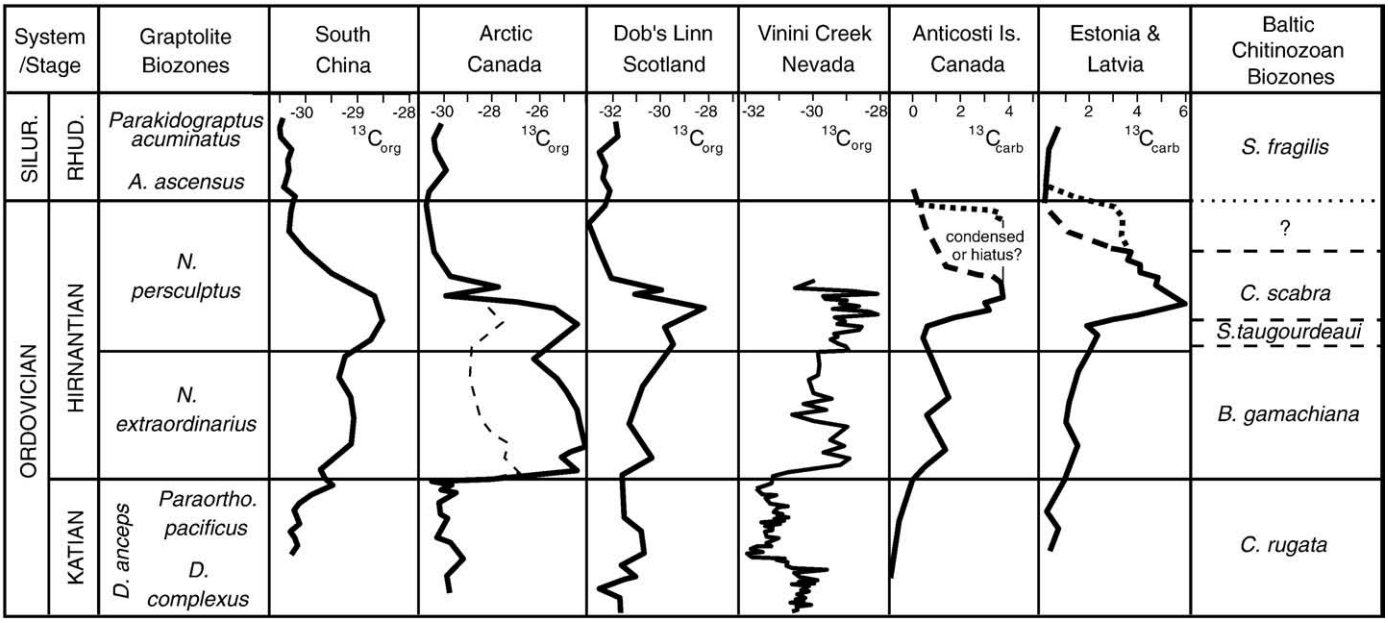

Fig. 6. Global correlation of the carbon isotope curves based on the graptolite and Baltic chitinozoan biozonation (after Melchin and Holmden, 2006). Sources of carbon isotope data: South China — this study; Arctic Canada — Melchin and Holmden (2006) (thin dashed line indicates the reduced values seen at Truro Island); Dob's Linn, Scotland — Underwood et al. (1997); Vinini Creek, Nevada — Mitchell et al. (2007) (the curve of the *N. extraordinarius* Biozone is rescaled to fit the *N. extraordinarius*/*N. persculptus* zonal boundary); Anticosti Island — Long (1993), composite of data from two sections (dashed line indicate correlation supported by available biostratigraphic data, dotted line indicates correlation with a significant hiatus as proposed by Brenchley et al., 2003); Estonia and Latvia — Brenchley et al. (2003) (dashed line indicated correlation based on synchroneity of C-isotope profiles, dotted line is based on chitinozoan correlation assuming that the base of *S. fragilis* biozone coincides with the base of the Silurian, as proposed by Brenchley et al., 2003). Rhud. = Rhuddanian Stage; Silur. = Silurian System.

Melchin and Holmden (2006) already presented a revised global correlation of graptolite and chitinozoan biozonations and $\delta^{13}C$ curves, based on new biostratigraphic data from Scotland, Anticosti Island, and Arctic Canada, which is mostly followed here except more details from South China (new data from the present paper) and Vinini Creek, Nevada (new data from Mitchell et al., 2007) (Fig. 6).

5.2.1. Dob's Linn

At Dob's Linn, Scotland, which is the Global Stratotype Section and Point (GSSP) for the base of the Silurian System, it appears that a major, positive $\delta^{13}C_{org}$ excursion begins just above the Anceps Band E. Some recent studies indicate that the Anceps Band E should be assigned to *N. extraordinarius* Biozone due to the FAD of the zonal fossil, and the Extraordinarius Band should be assigned to the lower part of the *N. persculptus* Biozone due to the presence of two specimens of *N. persculptus* (Melchin et al., 2003). Thus, the positive carbon isotope excursion at Dob's Linn, starts near the base of the Hirnantian Stage, and reaches a peak 1.72 m below the Ordovician–Silurian boundary, 0.12 m below the base of the Birkhill Shale Formation, which occurs within the lower part of the *N. persculptus* Biozone.

Dob's Linn is now widely accepted to represent deep sea sediments deposited on oceanic crust, preserved in an accretionary prism setting (Leggett, 1987; Stone and Merriman, 2004). The strata in which the $\delta^{13}C$ excursion occurs are organic-poor mudstones interpreted by Armstrong and Coe (1997) to represent the time of glacial maximum.

5.2.2. Arctic Canada

Melchin and Holmden (2006) studied three sections in Arctic Canada for both $\delta^{13}C_{org}$ and $\delta^{13}C_{carb}$. Their data showed two peaks of $\delta^{13}C_{org}$ values, one beginning just below the base of the Hirnantian Stage and reaching highest values low in the *N. extraordinarius* Biozone, and the other within the lower part of the *N. persculptus* Biozone. The $\delta^{13}C_{carb}$ data also showed a positive excursion in the Hirnantian, but the signal was heavily modified by diagenesis and reworked, detrital carbonate input.

Melchin and Holmden (2006) found that the lower Hirnantian peak was slightly higher in magnitude than the one in the lower *N. persculptus* Biozone, and that both occurred within shallow-water siltstones within a succession otherwise dominated by deeper shelf carbonates and calcareous or dolomitic, graptolitic, organic-rich shales.

5.2.3. Anticosti Island, Canada

On Anticosti Island, there is a positive, $\delta^{13}C_{carb}$ excursion in the uppermost Ellis Bay Formation (Long, 1993). Melchin (2007) identified *Normalograptus minor* and *Normalograptus parvulus* approximately 15 m and 4 m, respectively, below the top of the Ellis Bay Formation. Both species have been previously reported from strata not lower than the *N. persculptus* Biozone, which suggests that the most significant positive $\delta^{13}C_{carb}$ excursion in the Anticosti succession is within the *N. persculptus* Biozone. Two weaker positive shifts can be recognized in the lower part of the Ellis Bay Formation, which, based on brachiopod data, may be lower Hirnantian (*N. extraordinarius* Biozone) (Copper, 2001; Jin and Copper, 2008; Melchin and Holmden, 2006). Although Young et al. (2005) suggested that the peak $\delta^{13}C_{carb}$ values on Anticosti Island occurred within a sea level highstand interval, previous sedimentological and biofacies studies (Long and Copper, 1987; Long, 1997; Zhang and Barnes, 2002) all suggest that the excursion occurs within the peak lowstand level within the Late Ordovician succession.

5.2.4. Baltica

C-isotope data from Estonia and Latvia record a large $\delta^{13}C_{carb}$ excursion (Brenchley et al., 2003). However, the correlation of the chitinozoan biozones and shelly faunas from this area with the graptolite biozonation are still uncertain. Brenchley et al. (2003) attempted to use the carbon isotope profile to correlate the chitinozoan biozonation with the graptolite biozonation globally and they considered that the *taugourdeaui* Biozone and *scabra* Biozone can be correlated with the whole Hirnantian Stage, indicating that the major positive $\delta^{13}C$ excursion in carbonates seen in Estonia and Latvia coincides with the lower part of the Hirnantian Stage.

On the other hand, Melchin and Holmden (2006) suggested that, if the chitinozoan biozones are correlative between Anticosti Island (Soufiane and Achab, 2000) and Baltica (Nõlvak, 1999), on Anticosti Island most of the *Belonechitina gamachiana* chitinozoan Biozone (Soufiane and Achab, 2000) is lower Hirnantian (in the *N. extraordinarius* Biozone) and the uppermost *B. gamachiana* and *Spinachitina taugourdeaui* chitinozoan biozones are upper Hirnantian (in the *N. persculptus* Biozone). Therefore, the peak of the main positive C-isotope excursion and much the interval of rising C-isotope values observed in Estonia and Latvia (Brenchley et al., 2003), as well as Antocosti Island are within the *N. persculptus* Biozone. Brenchley et al. (2003) also showed that the positive $\delta^{13}C_{carb}$ excursion interval coincides with the occurrence of the *Hirnantia* fauna, which was demonstrated by Rong et al. (2002) to occur most widely in the upper *N. extraordinarius* and lower *N. persculptus* biozones.

Future work on the chitinozoan biozonation in South China, especially the Yichang area, may reveal a more precise correlation between chitnozoan biozones and graptolite biozones, as well as the carbon isotope curve.

5.2.5. Nevada

Two sections in Nevada, United States, were studied by Finney et al. (1999) for Late Ordovician graptolite, conodont, and chitinozoan biostratigraphy as well as the $\delta^{13}C_{carb}$ profile. In addition, new, high resolution $\delta^{13}C_{carb}$ and $\delta^{13}C_{org}$ data from one of the sections, Vinini Creek, were published by Mitchell et al. (2007). The Vinini Creek section shows continuous graptolite sequence from the *P. pacificus* Biozone into the *N. persculptus* Biozone. Although the $\delta^{13}C_{carb}$ and $\delta^{13}C_{org}$ curves show some differences in detail, both present a positive excursion beginning near the base of the *N. extraordinarius* Biozone with peak values occurring in the lower part of the *N. persculptus* Biozone. The upper part of the *N. persculptus* Biozone in this section is truncated by a disconformity and the overlying strata are middle Llandovery. Thus, the profile of the $\delta^{13}C$ curve in the upper *N. persculptus* Biozone and the lowest Silurian cannot be known.

The strata at Vinini Creek are interpreted to have been deposited on the deep ocean floor beyond the craton margin. The change from organic-rich shales to organic-poor limestones near the base of the Hirnantian is considered to be the result of sea level fall, coincident with the Gondwanan glaciation (Finney et al., 1995, 1999).

The Monitor Range section (Finney et al., 1999) shows a more complete succession of $\delta^{13}C_{carb}$ values, but the timing of the excursion relative to both the base of the *N. extraordinarius* Biozone and the *N. persculptus* Biozone is uncertain due to a lack of age-diagnostic fossil taxa through the lower-middle-Hirnantian. The succession does, however, indicate that the end of the positive excursion occurs below the top of the *N. persculptus* Biozone, which is not evident from the Vinini Creek data.

6. Discussion

6.1. Asynchronous stratigraphic distribution of peak $\delta^{13}C$ excursions

As indicated by Melchin and Holmden (2006), the attainment of peak $\delta^{13}C$ values may be offset between sedimentary deposits in different epeiric sea basins because of differences in the interplay between local and global influences on C-cycling. A detailed discussion on this can be found in Melchin and Holmden (2006, p. 196). The present data also support this theory. Although the organic $\delta^{13}C$ curve is similar to that from Arctic Canada, there are still some important differences. For example, both of them show separate peaks in the lower-mid-*N. extraordinarius* Biozone and the lower *N. persculptus* Biozone, but in the

Wangjiawan Riverside section, the highest peak occurs within the lower *N. persculptus* Biozone, whereas in Arctic Canada, the highest peak is in the *N. extraordinarius* Biozone. In this respect, the $\delta^{13}C$ curve at Wangjiawan resembles those of Dob's Linn (Underwood et al., 1997), Vinini Creek (Mitchell et al., 2007), Anticosti Island (Long, 1993), and Estonia and Latvia (Brenchley et al., 2003), where, according to Melchin and Holmden (2006), the excursions also begin near the base of the Hirnantian but reach their peak values in the lower part of the *N. persculptus* Biozone (Fig. 6).

The Wangjiawan Riverside section differs from other studied regions in that it only shows a maximum 2‰ positive excursion while the sections in Arctic Canada and elsewhere show a positive shift of 3–6‰. Melchin and Holmden (2006) proposed that these differences in magnitude of the $\delta^{13}C$ excursions are in part the result of the position of a particular section relative to the sedimentary basin margin, combined with differences in subsidence and sedimentation histories between different regions. At Wangjiawan, the shifts in the $\delta^{13}C$ curve closely follow the interpreted changes in regional sea level, with the highest values occurring at the time of maximum lowstand.

6.2. Timing and duration of the Hirnantian glaciation

Precise lithostratigraphic and biostratigraphic correlation between the Wangjiawan Riverside and the Wangjiawan North sections permits us to relate the timing of the $\delta^{13}C_{org}$ excursion and the GSSP for the Hirnantian Stage. As noted above, the positive excursion at Wangjiawan begins just below the base of the Hirnantian, reaches a peak within the lower Hirnantian *N. extraordinarius* Biozone, followed by a slight decline and then a higher peak within the lower part of the upper Hirnantian *N. persculptus* Biozone. $\delta^{13}C_{org}$ values then decline to pre-Hirnantian background levels before the end of the Hirnantian.

As discussed above, paleoecologic, lithologic, and paleogeographic evidence from South China suggests that a regional, continuous eustatic sea-level drop from the uppermost *P. pacificus* Biozone into the lower *N. persculptus* Biozone was brought about by the gradual growth of the ice sheet at the Ordovician South Pole region and ended with the rapid melting of the ice sheet. This provides indirect evidence for the timing of the Hirnantian glaciation. The record of glacial sediments in North Africa (Ghienne, 2003; Legrand, 2003) and Bohemia (Štorch, 2006) also indicates that the main phase of glaciation expansion began just before the beginning of the Hirnantian and finished before the end of Ordovician (Fig. 4). Based on recent estimates of the duration of the Hirnantian Stage and graptolite biozones (Cooper and Sadler, 2004; Chen et al., 2005), the duration of the Hirnantian glacial episode can be estimated to have been approximately 1 My.

The glacial record from Gondwanan and peri-Gondwanan regions also indicated that there were at least two main phases of glacial advance, one beginning at or just before the beginning of the Hirnantian, and one in mid-Hirnantian time (Ghienne, 2003; Legrand, 2003; Monod et al., 2003; Štorch, 2006). Each one of these episodes may have included two or more minor phases of glacial advance and retreat. Sedimentological data from peri-Gondwanan regions suggest that the second major glacial phase in the middle-Hirnantian was more intense, resulting in the greater eustatic sea-level drop (Monod et al., 2003; Štorch, 2006). This is consistent with the data from South China, which shows the lowest sea level and maximum $\delta^{13}C$ excursion in the Kuanyinchiao Bed, spanning the boundary between the *N. extraordinarius* and the *N. persculptus* biozones.

Saltzman and Young (2005) proposed a model of long-lived glaciation in the Late Ordovician (~10 Ma) beginning from the early Late Ordovician Chatfieldian Stage (Katian) based on $\delta^{13}C$ data from western Laurentia. They suggested that Gondwanan glacial ice buildup began in the Katian, but reached a peak expansion in Hirnantian time. The data from South China presented here do not span a sufficiently long stratigraphic interval to test this hypothesis, but do help to constrain the timing of the Hirnantian peak glacial episode in relation to the newly-defined Hirnantian stage, the graptolite biozonation, and the peak occurrence of the *Hirnantia* fauna. It should be noted, however, that both Boucot et al. (2003) and Fortey and Cocks (2005) presented strong evidence for a phase of significant climatic warming in high paleolatitude regions immediately before the Hirnantian glaciation event. This suggests that if continental glaciation did occur in the early part of the Late Ordovician, as suggested by Saltzman and Young (2005), it may have been a separate event, not continuous with the Hirnantian glaciation.

6.3. Causes of the positive $\delta^{13}C$ excursion and biotic recovery

There is currently debate in the literature concerning the causal relationship between the variations in $\delta^{13}C$ values and the glacial cycles in the Ordovician and Silurian. Whereas some authors have suggested that the $\delta^{13}C$ variations result from climatically driven changes in organic-matter productivity and burial patterns (e.g., Brenchley et al., 2003; Saltzman and Young, 2005), others have suggested that changes in rates of carbonate platform weathering were an important factor in generating the regionally variable record of $\delta^{13}C$ (e.g., Kump and Arthur, 1999; Kump et al., 1999; Melchin and Holmden, 2006), whilst Loydell (2007) proposed a combination of carbonate weathering and enhanced carbon burial coincident with falling/low sea-level. However, the data from the Truro Island, Arctic Canada (Melchin and Holmden, 2006, Fig. 2) and the Wangjiawan North section (Yan et al., 2009; Fig. 5 herein) both present two peaks in the TOC curve, the first at the base of the Hirnantian Stage and the second in the *N. persculptus* Biozone, while the TOC value between the two peaks is at the same level as in Katian. It is clear that the second peak in the TOC curve happened during the regression of the organic C-isotope excursion. Therefore, the data from the Truro Island and the Wangjiawan North section exclude the enhanced carbon burial model.

Cramer and Saltzman (2005), Saltzman and Young (2005), and Young et al. (2005) proposed that the positive $\delta^{13}C$ excursions of the Late Ordovician and Early Silurian, including the Hirnantian, occurred during times of post-glacial or interglacial sea level highstands. They suggested that during these non-glacial, warm, highstand periods there should be enhanced carbonate productivity in cratonic shelf regions, and high rates of burial of organic matter in stagnant deep-ocean settings, resulting in the increase in $\delta^{13}C$ values (called CSY Model here). However, the data from South China (this study) and Arctic Canada (Melchin and Holmden, 2006) clearly show that the $\delta^{13}C$ positive excursions coincide with sea level lowstands rather than highstands, as predicted by the CSY model and, as noted above, this appears to be the case at Anticosti Island as well. In addition, the data from two well-studied sections that represent deep ocean settings beyond the craton margin, Dob's Linn and Vinini Creek, indicate that the positive $\delta^{13}C$ excursion coincides with a time of reduced rates of organic matter burial in the deep ocean, rather than increased, as predicted by the CSY model.

Melchin and Holmden (2006) proposed that the $\delta^{13}C$ excursions are the result of increased rates of weathering of carbonate platforms that were exposed during the glacio-eustatically controlled sea-level fall. This caused the isotope value of the C-weathering flux to shift towards the ^{13}C-enriched carbonate end-member, increasing the $\delta^{13}C$ value of carbon transported by rivers to both epeiric seas and the oceans. The evidence of paleogeographic and sea-level changes from South China supports this hypothesis. Unlike the sedimentary basins studied in Baltica, Nevada, and Arctic Canada, which are adjacent to widespread carbonate platforms or shelves, the margins of the Yangtze Basin do not appear to have been sites of widespread carbonate deposition (Chen et al., 2004b). Therefore, the Hirnantian sea level fall would not have resulted in exposure and weathering of large volumes of recently deposited carbonate sediments. This may explain why the magnitude of the peak positive excursion in this section is lower than that in most other studied, low latitude regions. The approximately 2‰ shift seen in

these strata is similar to those seen in deep ocean strata deposited far from carbonate platforms in other regions (e.g. Underwood et al., 1997; Mitchell et al., 2007), and may represent the $\delta^{13}C$ values that were mixed throughout the world's oceans during this time interval (Melchin and Holmden, 2006).

7. Conclusions

The organic carbon isotope data through the Ordovician–Silurian boundary strata at the Wangjiawan Riverside section show that a positive $\delta^{13}C_{org}$ excursion begins just below the base of the Hirnantian Stage that peaks in the lower part of the *N. extraordinarius* Biozone. This is followed by an interval of slightly reduced $\delta^{13}C$ values and then a second peak of 2‰ above pre-Hirnantian values, which occurs in the lower part of the *N. persculptus* Biozone (upper Hirnantian).

The peaks in $\delta^{13}C_{org}$ values can be correlated well with major episodes of glacial expansion described from Africa and peri-Gondwanan Europe. Evidence from sedimentological, faunal, and geochemical data from South China, as well as the evidence of glacial sediments in North Africa, all suggest a short-lived glaciation of ~1 My in the Ordovician South Pole region, consisting of two major pulses. The first phase of glaciation commenced just before the Hirnantian Epoch and the second phase ended with rapid melting in the late Hirnantian (lower *N. persculptus* Biozone).

Carbon isotope curves can be correlated globally, providing useful data for recognition of Hirnantian strata. However, the timing and amplitude of peak positive excursions vary between regions of the world.

The present study supports the hypothesis by Melchin and Holmden (2006) that the $\delta^{13}C$ excursions are, to a significant extent, the result of increased rates of weathering of carbonate platforms that were exposed during the glacio-eustatically controlled sea-level fall. The low magnitude of the positive $\delta^{13}C$ shift seen from the Wangjiawan strata may be the result of a scarcity of carbonate platform strata in Katian successions of the Yangtze region, in comparison with other regions that show stronger positive excursions.

Acknowledgements

The present work is supported by the Chinese Academy of Sciences (KZCX2-YW-122 and KZCX3-SW-149), the Ministry of Science and Technology of China (2006CB806400) and the National Natural Science Foundation of China (40532009 and 40772002), and a Natural Sciences and Engineering Research Council of Canada Discovery Grant to MJM. We thank St. Francis Xavier University for providing a James Chair Professorship to FJX. We also thank Prof. Chen Xu for valuable suggestions on the manuscript. This paper benefited considerably from the constructive reviews of David Loydell and an anonymous reviewer. This is a contribution to the Geobiodiversity Database project (www.geobiodiversity.com) and IGCP 503 'Ordovician Palaeogeography and Palaeoclimate'.

References

Armstrong, H.D., Coe, A.L., 1997. Deep-sea sediments record the geophysiology of the Late Ordovician glaciation. Journal of the Geological Society (London) 154, 929–934.
Boucot, A., 1975. Evolution and extinction rate controls. Developments in Palaeontology and Stratigraphy, 1Elsevier, New York.
Boucot, A.J., Rong, J.-Y., Chen, X., Scotese, C.R., 2003. Pre-Hirnantian ashgill climatically warm event in the Mediterranean region. Lethaia 36 (2), 119–131.
Brenchley, P.J., Marshall, J.D., Carden, G.A.F., Robertson, D.B.R., Long, D.G.F., Meidla, T., Hints, L., Anderson, T.F., 1994. Bathymetric and isotopic evidence for a short lived Late Ordovician glaciation in a greenhouse period. Geology 22, 295–298.
Brenchley, P.J., Carden, G.A., Hints, L., Kaljo, D., Marshall, J.D., Martma, T., Meidla, T., Nolvak, J., 2003. High-resolution stable isotope stratigraphy of Upper Ordovician sequences: constraints on the timing of bioevents and environmental changes associated with mass extinction and glaciation. Bulletin of Geological Society of America 115 (1), 89–104.
Chen, X., Rong, J.Y., Mitchell, C.E., Harper, D.A.T., Fan, J.X., Zhan, R.B., Zhang, Y.D., Li, R.Y., Wang, Y., 2000. Late Ordovician to earliest Silurian graptolite and brachiopod biozonation from the Yangtze region, South Chian with a global correlation. Geological Magazine 137 (6), 623–650.
Chen, X., Fan, J.X., Melchin, M.J., Mitchell, C.E., 2004a. Patterns and processes of latest Ordovician graptolite extinction and survival in South China. In: Rong, J.Y., Fang, Z.J. (Eds.), Mass Extinction and Recovery — Evidences from the Palaeozoic and Triassic of South China. University of Science and Technology of China Press, Hefei, pp. 9–54. 1037–1038 (in Chinese, with English abstract).
Chen, X., Rong, J.Y., Li, Y., Boucot, A.J., 2004b. Facies patterns and geography of the Yangtze region, South China, through the Ordovician and Silurian transition. Palaeogeography, Palaeoclimatology, Palaeoecology 204, 353–372.
Chen, X., Melchin, M.J., Sheets, H.D., Mitchell, C.E., Fan, J.X., 2005. Patterns and processes of latest Ordovician graptolite extinction and recovery based on data from South China. Journal of Palaeontology 79 (5), 842–861.
Chen, X., Rong, J.Y., Fan, J.X., Zhan, R.B., Mitchell, C.E., Harper, D.A.T., Melchin, M.J., Peng, P.A., Finney, S.C., Wang, X.F., 2006. The Global boundary Stratotype Section and Point (GSSP) for the base of the Hirnantian Stage (the uppermost of the Ordovician System). Episodes 29 (3), 183–196.
Cooper, R.A., 1999. Ecostratigraphy, zonation and global correlation of earliest Ordovician planktic graptolites. Lethaia 32, 1–16.
Cooper, R.A., Sadler, P.M., 2004. Ordovician system. In: Gradstein, F.M., Ogg, J.G., Smith, A.G. (Eds.), A Geologic Time Scale. Cambridge University Press, Cambridge, pp. 165–187.
Cooper, R.A., Fortey, R.A., Lindholm, K., 1991. Latitudinal and depth zonation of early Ordovician graptolites. Lethaia 24, 199–218.
Copper, P., 2001. Reefs during the multiple crises towards the Ordovician–Silurian boundary: Anticosti Island, eastern Canada, worldwide. Canadian Journal of Earth Sciences 38, 153–171.
Cramer, B.D., Saltzman, M.R., 2005. Sequestration of ^{12}C in the deep ocean during the early Wenlock (Silurian) positive carbon isotope excursion. Palaeogeography, Palaeoclimatology, Palaeoecology 219, 333–349.
Fan, J.X., Chen, X., 2007. Preliminary report on the Late Ordovician graptolite extinction in the Yangtze region. Palaeogeography, Palaeoclimatology, Palaeoecology 245, 82–94.
Finney, S.C., Berry, W.B., 1997. New perspectives on graptolite distributions and their use as indicators of platform margin dynamics. Geology 25 (10), 919–922.
Finney, S.C., Berry, W.B.N., Sweet, W.C., 1995. An important Ordovician/Silurian boundary interval section in the Vinini Formation, Roberts Mountains, Nevada. In: Cooper, J.D., Droser, M.L., Finney, S.C. (Eds.), Ordovician Odyssey, Short Papers for the Seventh Annual International Symposium on the Ordovican System: Pacific Section, SEPM (Society for Sedimentary Geology), pp. 163–164. Book 77.
Finney, S.C., Berry, W.B.N., Cooper, J.D., Ripperdan, R.L., Sweet, W.C., Jacobson, S.R., Soufiane, A., Achab, A., Noble, P.J., 1999. Late Ordovician mass extinction: a new perspective from stratigraphic sections in central Nevada. Geology 27 (3), 215–218.
Fortey, R.A., Cocks, L.R.M., 2005. Late Ordovician global warming — the Boda event. Geology 33 (5), 405–408.
Ghienne, J.-F., 2003. Late Ordovician sedimentary environments, glacial cycles, and post-glacial transgression in the Taoudeni Basin, West Africa. Palaeogeography, Palaeoclimatology, Palaeoecology 189, 117–145.
Harper, D.A.T., Rong, J.Y., 1995. Patterns of change in the brachiopod faunas through the Ordovician–Silurian interface. Modern Geology 20, 83–100.
Jablonski, D., 1991. Extinctions: a paleontological perspective. Science 253, 754–756.
Jin, J., Copper, P., 2008. Response of brachiopod communities to environmental change during the Late Ordovician mass extinction interval, Anticosti Island, eastern Canada. Fossils and Strata 54, 41–51.
Kump, L.R., Arthur, M.A., 1999. Interpreting carbon-isotope excursions: carbonates and organic matter. Chemical Geology 161, 181–198.
Kump, L.R., Arthur, M.A., Patzkowski, M.E., Gibbs, M.T., Pinkus, D.S., Sheehan, P.M., 1999. A weathering hypothesis for glaciation at high atmospheric p_{CO2} during the Late Ordovician. Palaeogeography, Palaeoclimatology, Palaeoecology 152, 173–187.
Leggett, J.K., 1987. The Southern Uplands as an accretionary prism: the importance of analogues in reconstructing palaeogeography. Journal of the Geological Society, London 144, 737–752.
Legrand, P., 2003. Paléogéographie du Sahara algérien à l'Ordovicien terminal et au Silurien inférieur. Bulletin de la Société géologique de France 174 (1), 19–32.
Long, D.G.F., 1993. Oxygen and carbon isotopes and event stratigraphy near the Ordovician–Silurian boundary, Anticosti Island, Quebec. Palaeogeography, Palaeoclimatology, Palaeoecology 104, 49–59.
Long, D.G.F., 1997. Seven million years of storm redistribution along the east coast of Laurentia: transport mechanisms, current systems and influence of siliciclastics on reef development in the Late Ordovician and Early Silurian carbonate ramp of Anticosti Island, Quebec, Canada. Proceedings of the Eighth International Coral Reef Symposium 2, 1743–1748.
Long, D.G.F., Copper, P., 1987. Stratigraphy of the Upper Ordovician upper Vaureal and Ellis Bay formations, eastern Anticosti Island, Quebec. Canadian Journal of Earth Sciences 24, 1807–1820.
Loydell, D.K., 2007. Early Silurian positive $\delta^{13}C$ excursions and their relationship to glaciations, sea-level changes and extinction events. Geological Journal 42, 531–546.
Melchin, M.J., 2007. Restudy of some Ordovician–Silurian boundary graptolites from Anticosti Island, Canada, and their biostratigraphic significance. Lethaia 41 (2), 155–162.
Melchin, M.J., Holmden, C., 2006. Carbon isotope chemostratigraphy in Arctic Canada: Sea-level forcing of carbonate platform weathering and implications for Hirnantian global correlation. Palaeogeography, Palaeoclimatology, Palaeoecology 234, 186–200.
Melchin, M.J., Holmden, C., Williams, S.H., 2003. Correlation of graptolite biozones, chitinozoan biozones, and carbon isotope curves through the Hirnantian. In: Albanesi, G.L., Beresi, M.S., Peralta, S.H. (Eds.), Ordovician from the Andes. INSUGEO, serie Correlación Geologica, vol. 17, pp. 101–104.
Mitchell, C.E., Sheets, H.D., Belcher, K., Finney, S.C., Holmden, C., Laport, D., Melchin, M., Patterson, W.P., 2007. Species abundance changes during mass extinction and the

inverse Signor–Lipps effect: apparently abrupt graptolite mass extinctions as an artifact of sampling. Acta Palaeontologica Sinica 46 (Suppl.), 340–346.
Monod, O., Kozlu, H., Ghienne, J.-F., Dean, W.T., Günay, Y., Hérissé, A.L., Paris, F., Robardet, M., 2003. Late Ordovician glaciation in southern Turkey. Terra Nova 15 (4), 249–257.
Mu, E.Z., Zhu, Z.L., Lin, Y.K., Wu, H.J., 1984. The Ordovician–Silurian boundary in Yichang, Hubei. Stratigraphy and palaeontology of systemic boundaries in China. In: Nanjing Institute of Geology and Palaeontology (Ed.), Stratigraphy and Palaeontology of Systemic Boundaries in China, 1. Ordovician – Silurian Boundary. Anhui Science and Technology Publishing House, Hefei, pp. 15–44.
Mu, E.Z., Li, J.J., Ge, M.Y., Chen, X., Lin, Y.K., Ni, Y.N., 1993. Upper Ordovician graptolites of central China region. Palaeontologia Sinica, B 29, 1–393 (in Chinese, with English summary).
Nõlvak, J., 1999. Ordovician chitinozoan biozonation of Baltoscandia. Acta Universitatis Carolinae-Geologica 43 (1/2), 287–290.
Rong, J.Y., 1979. The Hirnantia Fauna of China with the comments on the Ordovician-Silurian Boundary. Acta Stratigraphica Sinica 3 (1), 1–29.
Rong, J.Y., 1984a. Distribution of the Hirnantia fauna and its meaning. In: Bruton, D.L. (Ed.), Aspects of the Ordovician System. Palaeontological Contributions from the University of Oslo, vol. 295, pp. 101–112.
Rong, J.Y., 1984b. Brachiopods of latest Ordovician in the Yichang District, western Hubei, Central China. In: Nanjing Institute of Geology and Palaeontology, Academia Sinica (Ed.), Stratigraphy and Palaeontology of Systemic Boundaries in China. v. 1, Ordovician-Silurian Boundary. Anhui Science and Technology Publishing House, Hefei, pp. 111–176.
Rong, J.Y., Chen, X., 1987. Faunal differentiation, biofacies and lithofacies pattern of Late Ordovician (Ashgillian) in South China. Acta Paleontologica Sinica 26, 507–535 (in Chinese, with English summary).
Rong, J.Y., Harper, D.A.T., 1988. A global synthesis of the latest Ordovician Hirnantian brachiopod faunas. Transactions of the Royal Society of Edinburgh, Earth Science 79, 383–402.
Rong, J.Y., Johnson, M.E., 1996. A stepped karst unconformity as an Early Silurian rocky shoreline in Guizhou Province (South China). Palaeogeography, Palaeoclimatology, Palaeoecology 121, 115–129.
Rong, J.Y., Zhan, R.B., 2004. Late Ordovician brachiopod mass extinction of South China. In: Rong, J.Y., Fang, Z.J. (Eds.), Mass Extinction and Recovery — Evidences from the Palaeozoic and Triassic of South China. University of Science and Technology of China Press, Hefei, pp. 71–96. 1040 (in Chinese, with English abstract).
Rong, J.Y., Johnson, M.E., Yang, X.C., 1984. Early Silurian (Llandovery) sea-level changes in the Upper Yangzi region of central and southwestern China. Acta Palaeontologica Sinica 23, 672–694 (in Chinese, with English abstract).
Rong, J.Y., Zhan, R.B., Harper, D.A.T., 1999. Late Ordovician (Caradoc–Ashgill) brachiopod faunas with Foliomena based on data from China. Palaios 14, 412–431.
Rong, J.Y., Chen, X., Harper, D.A.T., 2002. The latest Ordovician Hirnantia Fauna (Brachiopoda) in time and space. Lethaia 35, 231–249.
Rong, J.Y., Fan, J.X., Li, G.X., Miller, A.I., 2007. Dynamic patterns of latest Proterozoic–Palaeozoic–early Mesozoic Ediacaran to Triassic marine biodiversity in South China. Geological Journal 42, 431–454.
Saltzman, M.R., Young, S.A., 2005. Long-lived glaciation in the Late Ordovician? Isotopic and sequence-stratigraphic evidence from western Laurentia. Geology 33 (2), 109–112.
Sheehan, P.M., 2001. The Late Ordovician mass extinction. Annual Reviews of Earth and Planetary Sciences 29, 331–364.
Soufiane, A., Achab, A., 2000. Chitinozoan zonation of the Late Ordovician and the Early Silurian of the island of Anticosti, Quebec,Canada. Review of Palaeobotany and Palynology 109, 85–111.
Stone, P., Merriman, R.J., 2004. Basin thermal history favours an accretionary origin for the Southern Uplands terrane, Scottish Caledonides. Journal of the Geological Society 161, 829–836.
Štorch, P., 2006. Facies development, depositional settings and sequence stratigraphy across the Ordovician–Silurian boundary: a new perspective from the Barrandian area of the Czech Republic. Geological Journal 41, 163–192.
Underwood, C.J., Crowley, S.F., Marshall, J.D., Brenchley, P.J., 1997. High-resolution carbon isotope stratigraphy of the basal Silurian Stratotype (Dob's Linn, Scotland) and its global correlation. Journal of the Geological Society, London 154, 709–718.
Wang, X.F., Ni, S.Z., Zeng, Q.L., Xu, G.H., Zhou, T.M., Li, Z.H., Xiang, L.W., Lai, C.G., 1987. Biostratigraphy of the Yangtze Gorge area 2: Early Palaeozoic Era. Geological Publishing House, Beijing. (in Chinese).
Wang, K., Chatterton, B.D.E., Wang, Y., 1997. An organic carbon isotope record of Late Ordovician to Early Silurian marine sedimentary rocks, Yangtze Sea, South China: Implications for CO_2 changes during the Hirnantian glaciation. Palaeogeography, Palaeoclimatology, Palaeoecology 132, 147–158.
Yan, D.T., Chen, D.Z., Wang, Q.C., Wang, J.G., Wang, Z.Z., 2009. Carbon and sulfur isotopic anomalies across the Ordovician-Silurian boundary on the Yangtze platform, South China. Palaeogeography, Palaeoclimatology, Palaeoecology 274, 32–39.
Young, S.A., Saltzman, M.R., Bergström, S.A., 2005. Late Ordovician (Mohawkian) carbon isotope ($\delta^{13}C$) stratigraphy in Eastern and Central North America: regional expression of a perturbation of the global carbon cycle. Palaeogeography, Palaeoceanography, Palaeoclimatology 222, 53–76.
Zhan, R.B., Rong, J.Y., 1995. Synecology and their distribution pattern of Late Ordovician brachiopods from the Zhejiang–Jiangxi border region, E. China. Chinese Bulletin of Sciences 40, 923–935 (in Chinese).
Zhan, R.B., Cocks, L.R.M., 1998. Late Ordovician brachiopods from the South China Plate, and their palaeobiogeographical significance. Special Paper in Palaeontology 59, 5–70.
Zhang, S.X., Barnes, C.R., 2002. Eustatic sea level curve for the Ashgillian–Llandovery derived from conodont community analysis, Anticosti Island, Québec. Palaeogeography, Palaeoclimatology, Palaeoecology 180, 5–32.